UC Irvine
UC Irvine Previously Published Works

Title
Seasonal Patterns of Riverine Carbon Sources and Export in NW Greenland

Authors
Csank, Adam Z
Czimczik, Claudia I
Xu, Xiaomei
et al.

Key Points:
- Rivers in NW Greenland transport $4.5–8.2 \times 10^{-5}$ Tg C/year of dissolved organic carbon with the majority exported early in the melt season
- Seasonally, sources shift from young, plant-like carbon from forelands to older, more processed carbon from glaciers, soils, and sediments
- Based on modeled discharge, we estimate a carbon flux of 0.29% to $0.45\% \pm 20\%$ Tg C/year for Greenland, 35–40% higher than previous estimates

Correspondence to:
A. Z. Csank,
acsank@unr.edu

Author Contributions:
Conceptualization: Claudia I. Czimczik, Jeffrey M. Welker
Data curation: Adam Z. Csank
Formal analysis: Adam Z. Csank, Claudia I. Czimczik, Xiaomei Xu
Funding acquisition: Claudia I. Czimczik, Jeffrey M. Welker
Investigation: Adam Z. Csank, Claudia I. Czimczik, Jeffrey M. Welker
Methodology: Adam Z. Csank, Claudia I. Czimczik, Xiaomei Xu, Jeffrey M. Welker
Project administration: Adam Z. Csank, Claudia I. Czimczik, Jeffrey M. Welker
Resources: Adam Z. Csank
(continued)

Seasonal Patterns of Riverine Carbon Sources and Export in NW Greenland

Adam Z. Csank[1] (iD), **Claudia I. Czimczik[2]** (iD), **Xiaomei Xu[2]** (iD), and **Jeffrey M. Welker[3,4]** (iD)

[1]Department of Geography, University of Nevada, Reno, NV, USA, [2]Department of Earth System Science, University of California, Irvine, CA, USA, [3]Department of Biological Sciences, University of Alaska, Anchorage, AK, USA, [4]UArctic and Ecology and Genetics Research Unit, University of Oulu, Oulu, Finland

Abstract Glacial runoff exports large amounts of carbon (C) to the oceans, but major uncertainty remains regarding sources, seasonality, and magnitude. We apportioned C exported by five rivers from glacial and periglacial sources in northwest Greenland by monitoring discharge, water sources (δ^{18}O), concentration and composition of dissolved organic carbon (DOC), and ages (^{14}C) of DOC and particulate organic C over three summers (2010–2012). We found that particulate organic C ($F = 1.0366–0.2506$) was generally older than DOC in glacial sourced rivers and likely sourced from the physical erosion of aged C pools. Most exported DOC showed strong seasonal variations in sources and discharge. In summer, mean DOC ages ranged from modern to 4,750 cal years BP ($F = 1.0022–0.6291$); however, the annual C flux from glacially sourced rivers was dominated by young, plant-derived DOC ($F = 0.9667–1.002$) exported during the spring freshet. The most aged DOC ($F = 0.6891–0.8297$) was exported in middle to late summer at lower concentrations and was glacial in origin. Scaled to the whole of Greenland using model-estimated runoff, we estimate a total riverine DOC flux of 0.29% to $0.45\% \pm 20\%$ Tg C/year. Our flux results indicate that the highest C fluxes occur during the time of year when the majority of C is modern in age. However, higher melt rates from the Greenland ice sheet and longer growing seasons could result in increasing amounts of ancient C from the Greenland ice sheet and from the periglacial landscape to the ocean.

1. Introduction

Surface waters in the Arctic Ocean have the highest concentrations of dissolved and particulate organic carbon (C; DOC and POC, respectively) of any ocean basin (Amon, 2004; Benner et al., 2005; McClelland et al., 2012). This is a consequence of northern rivers draining Arctic and boreal landscapes underlain by permafrost (Neff et al., 2006; Raymond et al., 2007), which hold 30–50% of the world's soil C stocks (Hugelius et al., 2014).

Today, the Arctic is undergoing rapid and dramatic changes as a result of climate warming (Serreze & Barry, 2011; Timmermans et al., 2018) and wetting (Bintanja & Selten, 2014), including shifts in permafrost distribution (Romanovsky et al., 2010) as well as vegetation productivity and composition (e.g., Elmendorf et al., 2012). We are also observing accelerated export of C from land and glaciers to rivers, lakes, and oceans (e.g., Hood et al., 2009; Kicklighter et al., 2013; Lawson et al., 2014; Neff et al., 2006; Spencer et al., 2015) along with changes in the magnitude and balance of land-atmosphere C fluxes (e.g., Blanc-Betes et al., 2016; Commane et al., 2017; Lupascu et al., 2014).

The current and future extent of land-sea C fluxes is especially uncertain around the Greenland ice sheet (GIS), where an estimated $0.08–0.17 \pm 0.02$ Pg C/year enters the surrounding seas (Baffin Bay, Barents Sea, Kane Basin, and Karl Sea) and the Arctic Ocean (Bhatia et al., 2013; Hilton et al., 2015; Lawson et al., 2014). Atmospheric warming (Hanna et al., 2012) and ocean heat transport (Rignot et al., 2010) are contributing to GIS melt and thinning along the margins (Rignot et al., 2008). There have recently been years when the entire ice sheet surface undergoes melt (Mote, 2007; Nghiem et al., 2012), resulting in noticeable changes in river discharge and chemistry (Bhatia et al., 2011; Lawson et al., 2014).

Glacial runoff is an important mechanism for the export of organic C to the oceans (e.g., Bhatia et al., 2013; Hood et al., 2015; Lawson et al., 2014; Zhu et al., 2016). Sources of this glacial C are the deposition of aerosols, including pyrogenic C (e.g., McConnell et al., 2007; Mouteva et al., 2015; Stubbins et al., 2012; Tedesco et al., 2016), the drainage and erosion of subglacial C reservoirs (Bhatia et al., 2013), and in situ microbial activity on, within, and below the GIS (Bhatia et al., 2010, 2013; Hood et al., 2015, 2009). Because this glacial C

Supervision: Claudia I. Czimczik, Xiaomei Xu, Jeffrey M. Welker
Validation: Claudia I. Czimczik
Visualization: Adam Z. Csank, Claudia I. Czimczik
Writing - original draft: Adam Z. Csank, Claudia I. Czimczik
Writing – review & editing: Adam Z. Csank, Claudia I. Czimczik, Xiaomei Xu, Jeffrey M. Welker

consists of up to 10% carbohydrates, it may also serve as a substrate for in-stream organisms and organisms at the base of the adjacent near-shore marine food web (Lawson et al., 2014).

At the same time, the surrounding periglacial land surface has large stores of ancient C (Burnham & Sletten, 2010; Hågvar & Ohlson, 2013), some of which is diffusing into the modern atmosphere (Lupascu, Welker, Seibt, Xu, et al., 2014) and some that may be dissolved in surface waters, transported to rivers, and discharged into the Arctic Ocean. We do not fully understand, nor have we quantified, the interannual fluctuations in the sources of C in NW Greenland rivers that are simultaneously transporting ice sheet melt water and adjoining terrestrial-based soil water into Baffin Bay.

Currently, the GIS contributes a significant amount of meltwater runoff to the surrounding coastal environment, equivalent to the average annual discharge from a large Arctic river (e.g., the Ob River), and meltwater fluxes continue to increase with ongoing Arctic warming (Bamber et al., 2012; Bhatia et al., 2013; Yang et al., 2016). Although at present these meltwater and discharge changes have yet to alter major ocean circulation patterns (Tedesco et al., 2016), they may be influencing the nearshore food web (Causey et al., 2014).

Here we measured seasonal changes in the concentration, composition, and radiocarbon (^{14}C) content of DOC and POC in glacially sourced and nonglacially sourced periglacial rivers to quantify the relative contributions of glacial and periglacial C sources to the current riverine C flux in NW Greenland over three summers.

2. Materials and Methods

We monitored riverine C export near U.S. Air Force Base Thule on the northwestern margin of the GIS (76°31′48″N; 68°42′21″W). Samples were collected between May and August from 2010 to 2012 along four glacially sourced rivers (Fox Canyon, North, Narssarssuk, and Green Valley Rivers) and one periglacial river with no connection to the GIS (North Mountain River; Figure 1). To understand the sources of runoff and their C loads and sources, water samples were analyzed for their isotopic composition (δ^{18}O), the concentrations and molecular composition of DOC, and the C isotopic compositions (Δ^{14}C and δ^{13}C) of DOC and POC.

2.1. River Systems
2.1.1. Glacially Sourced Rivers
Fox Canyon River flows for 14 km from its source at the GIS to its delta at Northstar Bay. Over the 3 years of our study, we sampled Fox Canyon River at three locations for total DOC concentrations: at its source at the GIS (FCS, monthly), its midpoint where the river is crossed by a bridge (FCB, biweekly), and its delta at Northstar Bay (FCD, biweekly). We also collected samples for C isotope analysis of DOC and POC monthly at FCS and biweekly at FCB; the reduced sampling interval was because of the extra time required for sample processing.

North River originates at the GIS and is the largest river in the area by discharge. It flows through the center of Thule, and its lower catchment is heavily influenced by human activities. In 2012, we sampled North River approximately 2 km downstream of its origin at the GIS for both DOC concentration and isotope analysis (NR5, biweekly). In all 3 years of our study, we also sampled North River for DOC concentration at a location on base at the midpoint of the river where it is crossed by a bridge (NRB, biweekly).

Episodically, we also sampled two other glacially sourced rivers for DOC concentration and DOC and POC C isotopes: (1) Narssarssuk River (2011 and 2012), located approximately 15 km southwest of Thule, and (2) Green Valley River (2010 and 2011), located approximately 30 km southeast of Thule near the Pittufik glacier. These remote rivers were included because they provide important examples of different fluvial systems found in the region. The Narssarssuk River is sourced from a small glacier that is separate from the GIS. Its watershed is sparsely vegetated and represents a polar desert. The Green Valley River originates at the GIS, and its watershed is unusually productive due to nutrient inputs from sea bird colonies located in the valley (Causey et al., 2014).

2.1.2. Nonglacially Sourced River
The periglacial North Mountain River flows north–east from its source in a series of periglacial lakes and is one of the few fluvial systems in the area with no connection to the GIS. Our sampling site is in proximity to
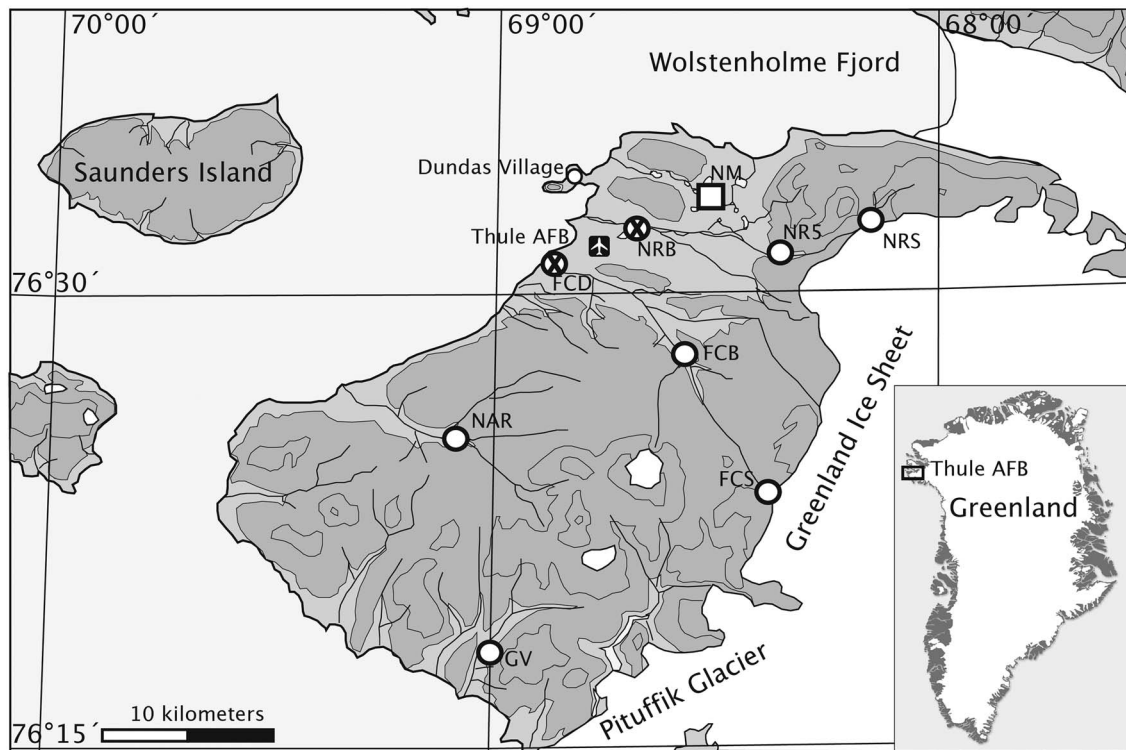
Figure 1. Map showing the water sampling locations in NW Greenland at which the concentrations and isotopic composition of DOC and/or POC were monitored, along with the isotopic composition of the water ($\delta^{18}O$). Sites not analyzed for POC are marked as (X). Circles indicate glacially sourced rivers: Fox Canyon at source (FCS), bridge (FCB), or delta (FCD); North River at source (NRS), shelter 5 (NR5), or bridge (NRB); Narssarssak River (NAR); and Green Valley River (GV). Square indicates nonglacially sourced river: North Mountain River (NM).

an experimental site where we were examining soil C responses to experimental warming and wetting (Lupascu, Welker, Seibt, Xu, et al., 2014; Sharp et al., 2013; Sullivan et al., 2008).

2.2. Climate

The mean annual air temperature at Thule airport is -11.4 ± 1.3 °C, with a mean annual precipitation of 122.6 ± 45.4 mm (1952–2012). Approximately 50% of the precipitation falls as snow between October and April. In summer, the majority of precipitation events occur in July and August. During our study period (2010–2012), average summer air temperature was highest in 2011, with summer temperatures on average 2 °C above normal (Figure 2). Total precipitation was above normal in both 2012 and 2010 and below normal in 2011. The wettest summer was 2012, with 161.3 mm of precipitation (Lupascu, Welker, Seibt, Xu, et al., 2014).

2.3. Sample Collection and Analysis
2.3.1. Discharge and Water Sources

Discharge was monitored in two of our rivers: episodically (measured biweekly) at Fox Canyon using a current velocity meter (Swoffer, Seattle, WA, USA) and continuously at North Mountain using a pressure transducer in the stream bed (Onset Computer Corporation, Bourne, MA, USA). At Fox Canyon we measured discharge at a bridge, which provided constraints on the channel shape. We measured at 12 points centered at 1-m intervals in a transect across the width of the bridge where we also measured depth to the channel. The relationship to the concrete river "bank" formed by the bridge was 90°. Time of measurement and air temperature were always recorded, and discharge was subsequently corrected for any diurnal variations by comparing the discharge measurements with a stationary stream height gauge maintained by R. Sletten (personal communication, August 2012) on a nearby river (North River). The pressure transducer used to measure discharge at North Mountain was calibrated through biweekly measurements of flow velocity and depth by using a current velocity flow meter and a ruler at two points centered at 1-m intervals across the channel. We also measured height to the pressure transducer and corrected the pressure
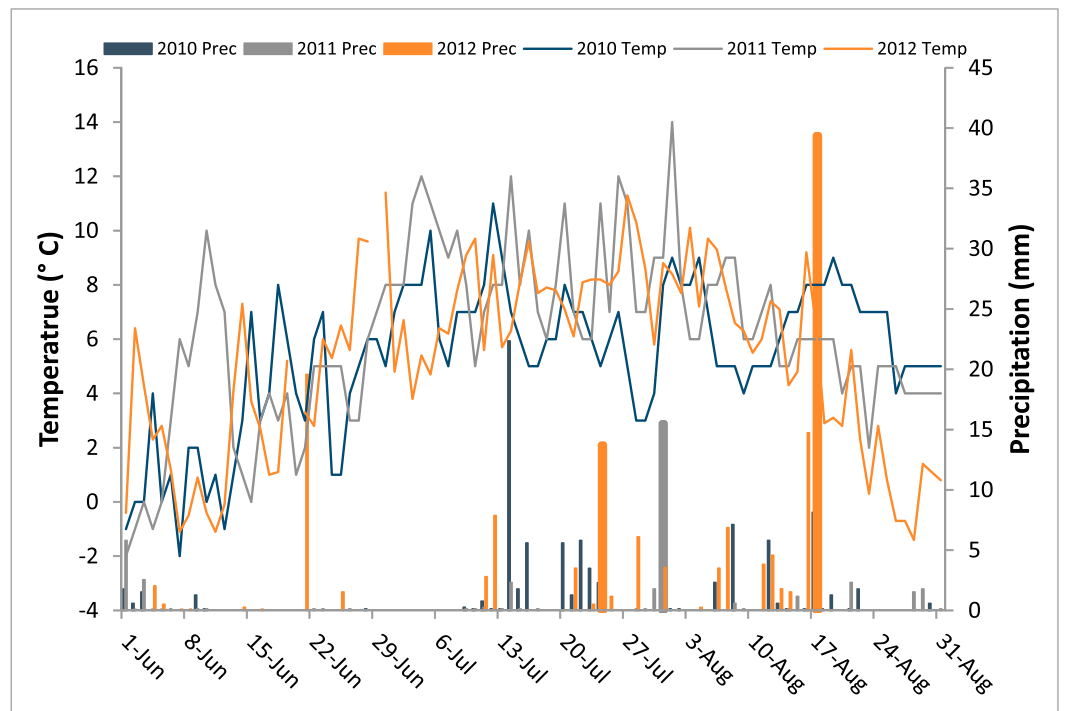
Figure 2. Summertime daily mean air temperature (lines) and daily total precipitation (bars) at Thule airport in 2010, 2011, and 2012.

transducer for the influence of variations in atmospheric pressure by using data from a subaerially installed pressure transducer on the stream bank. A linear regression was used to relate the biweekly discharge measurements to stream height above the pressure transducer, and this relationship was used to produce a continuous discharge curve for North Mountain.

To identify water sources, we also monitored the water isotopic composition (δ^{18}O) of the Fox Canyon and North Mountain Rivers along with that of precipitation and GIS runoff. River water isotope samples were collected in 10-ml Nalgene bottle concurrently with samples for DOC from each site. The water sampling interval varied from weekly to several times a season, depending on site access and sample processing time.

Meteoric rain and snow were collected throughout the summer at Thule using a bucket with samples transferred to a 10-ml Nalgene bottle and sealed with electrical tape at the end of each precipitation event. Snowpack was sampled from pits dug on North Mountain in May of 2011 and 2012 with samples collected every 20 cm. Samples were collected in 30-ml Nalgene bottles and sealed with electrical tape. The ice core collected on the GIS at Camp Century in the 1960s provided isotopic data for glacial ice by averaging the values over the entire core (Clausen et al., 1988; Dansgaard et al., 1969). Runoff from the GIS was collected in mid-July of 2011 and 2012 from an outflow off the GIS in 10-ml Nalgene bottles. All samples were analyzed for δ^{18}O using a Picarro cavity ring-down spectroscopy with an analytical precision of 0.03‰ at the University of Alaska, Anchorage.

2.3.2. Riverine Carbon Sources

To minimize contamination by extraneous C, prior to sampling all glassware was rinsed in deionized water, acid washed in 10% hydrochloric (HCl) acid, rinsed thoroughly with UV-treated Milli-Q water (Milli-Q Advantage A10, EMD Millipore, Billerica, MA, USA), and subsequently baked at 550 °C for 4 HR. Post baking bottle openings were sealed with Al foil, and bottles were stored in clean Ziploc bags for transport to the field sites. All Teflon, plastic, and silicone parts used in sample collection were also precleaned: rinsed in deionized water, soaked in 10% HCl, and rinsed extensively with Milli-Q water. In the field, all samples were collected in bottles rinsed with sample water prior to collection. All chemicals were trace-metal grade or better. Samples were generally collected in the morning. Preprocessing of samples was carried out in a field laboratory located at Thule.

Samples for DOC concentration analysis were collected in 250-ml amber glass bottles. All samples were filtered at our field laboratory within 2 hr of collection using a single-use 0.45-μm syringe filter (Whatman, GE Healthcare Bio-Sciences, Pittsburgh, USA) and then frozen and stored at −20 °C. Although it is possible that freezing DOC samples can introduce biases, including a reduction in DOC concentrations (Spencer et al., 2007), Fellman et al. (2008) found that for water samples with low DOC concentrations (<5 mg C/L) these biases are minimal. Blanks were produced by filling 250-ml amber glass bottles with Milli-Q water followed by filtering and then freezing. Samples and blanks were analyzed for DOC concentrations on a Shimadzu TOC-VCHN in the Applied Science, Engineering and Technology laboratory at the University of Alaska, Anchorage. The limit of detection, according to instrument blanks, was 0.02 mg C/L. Errors on DOC concentration values were 0.05 mg C/L, based on our field blanks.

Samples for dissolved and particulate organic ^{14}C (DO^{14}C and PO^{14}C, respectively) analyses were collected in 4-L amber glass bottles. DO^{14}C samples were acidified to pH 2 using concentrated HCl and filtered in our laboratory at Thule after collection using a combusted glass filtration apparatus, through a 0.7-μm precombusted quartz-fiber filter (Whatman). The filtrate was then frozen using a shell freezer (LabConco 79490, Kansas City, USA) and freeze dried using a Virtis benchtop freeze-dryer (SP Industries, New York, USA) to concentrate the DOC. Freeze-dried material was transferred to a 500-ml amber glass bottle for storage and transport. The glass-fiber filters containing PO^{14}C were placed in a 100-ml glass jar freeze-dried and stored at −20 °C prior to shipment. Field blanks and standards were prepared by dissolving a small amount of a ^{14}C-depleted and ^{14}C-enriched reference material (IAEA-C8–oxalic acid, $F = 0.1503$, or IAEA-C6–sucrose, $F = 1.5061$) in Milli-Q water to a concentration of 0.5–1.0 mg C/L, inside one of the same 4-L amber glass bottles used for sampling. These standards were subsequently acidified, filtered, and freeze-dried following the same method outlined above.

Radiocarbon analyses were carried out at the W.M. Keck Carbon Cycle Accelerator Mass Spectrometry (KCCAMS) laboratory at the University of California, Irvine (Beverly et al., 2010). DO^{14}C and PO^{14}C samples were converted to carbon dioxide (CO_2) by combustion with CuO in a vacuum-sealed double quartz tube (5-cm-long, 6-mm-outside-diameter quartz tube inside a 15.25 cm-long, 9-mm-outside-diameter quartz tube) at 900 °C for 2 hr. CO_2 was extracted and purified cryogenically and then graphitized by the sealed-tube Zn reduction method (Xu et al., 2007). Samples were processed alongside regular-sized and sample size-matched, double-tubed combusted standards (OX-I, IAEA-C6, and IAEA-C8) and blanks (^{14}C-free coal). The Accelerator Mass Spectrometry instrument measurement uncertainty is about 2–3‰ for regular-size (~1 mg C) modern samples based on long-term measurement of secondary standards. Based on the field standards and blanks, the uncertainty of the Δ^{14}C measurements was ~4–5‰. When samples were > 0.3 mg C, an aliquot of CO_2 gas was analyzed for δ^{13}C with a Gasbench II coupled with an isotope ratio mass spectrometry (Finnigan Delta Plus XL, Thermo Fisher Scientific, Pittsburgh, PA, USA). The uncertainty of the δ^{13}C analysis is ~0.15‰ based on long-term measurement of secondary standards.

A qualitative overview of the relative proportions of protein-like and humic-like fluorophores in DOC is allowed by spectrofluorometric measurements (Coble, 1996, 2007; Fellman et al., 2010). Protein-like compounds typically encompass amino-acid-rich, high-molecular-weight material indicative of microbial products/activity, while humic-like components are interpreted as proxies of vascular plants material. Fluorescence spectra were determined on a FluoroMax-4 (HORIBA Scientific, Irvine, CA, USA) spectrofluorometer at the University of Alaska, Anchorage. A 10-nm bandwidth and an 18-nm offset between excitation and emission monochromators were used following Barker et al. (2006). All scans were corrected for Ramen and Rayleigh scattering. We produced fluorescence excitation-emission matrices (EEMs) from each sample to identify what the dominant compounds in each measured sample were.

3. Results and Discussion

3.1. Flow Regimes

Based on climate data, discharge curves, and river water δ^{18}O values, we divided the discharge of the Fox and North Mountain rivers into three distinct regimes: snow melt (freshet) followed by (i) glacial melt and glacial melt mixed with rain in the glacially sourced rivers or (ii) baseflow and rain in the nonglacially sourced rivers (Table 1 and Figures 2 and 3). For the glacially sourced rivers, the end point of the snow melt

Table 1

Average $\delta^{18}O$ Values of Riverine Water and Regional Water Sources, Discharge, and Export of Dissolved Organic Carbon (DOC) by the Glacially Sourced Fox Canyon River and the Nonglacially Sourced North Mountain River in NW Greenland

X	$\delta^{18}O$ (‰)			Duration (day)		Precipitation (mm)		Discharge (m³/day)		DOC flux (kg C/day)	
	Mean	1 SD	*n*	Mean	1 SD	Mean	1 SD	Mean	1 SD	Mean	1 SD
Fox Canyon											
Snow melt (freshet)	−21.3	0.7	19	19	4	13.0	9.9	1.6×10^6	0.7×10^6	2178	2,034
Glacial melt/baseflow	−20.3	0.6	14	22	6	15.0	14.4	0.9×10^6	0.8×10^6	252	538
Mixed glacial/rain	−20.0	0.5	24	23[a]	4	59.1	41.1	0.6×10^6	0.5×10^6	324	414
North Mountain											
Snow melt (freshet)	−18.5	1.4	20	21	2	13.0	9.9	1.7×10^4	2.4×10^4	67	96
Baseflow	−16.7	0.7	15	22	2	15.0	14.4	0.9×10^4	0.1×10^4	8	7
Rain fed	−16.0	0.5	18	25[a]	2	59.1	41.1	0.6×10^4	0.1×10^4	26	45
Regional water sources											
Rain	−16.9	4.7	55	NA		NA		NA		NA	
Snow	−22.7	4.0	23	NA		NA		NA		NA	
Greenland ice sheet runoff	−20.5	1.0	64	NA		NA		NA		NA	

Note. Three flow regimes were identified for each river based the isotopic composition of the river water, the discharge, and precipitation (rain). NA = not applicable.
[a]We stopped sampling prior to freeze-up, so this is a minimum number of days.

period was defined as the point when the $\delta^{18}O$ values of the river water ceased increasing. For the nonglacially sourced river, the end of the snow melt period was defined as the point when the $\delta^{18}O$ values were no longer differentiable from precipitation. In the glacial Fox Canyon River, this point also coincided with when summer temperatures reach their maximum values. The start of the mixed glacial/rain and rain-fed periods was defined based on when most of the summer precipitation began falling (Figure 2). The majority (19–68%) of discharge to the ocean occurred in the first 2 weeks that the river started to flow.

In June, water in glacial-fed rivers was mostly derived from current year's snow, while the contribution from glacial melt and rain events increased as the season progresses. This was apparent in the GIS-sourced Fox Canyon River, where runoff exhibited depleted $\delta^{18}O$ values in the early part of the melt season and then increased and stabilized around mid-late June (Figure 3c and Table 2). It should, however, be noted that GIS melt is likely to consist of a mixture of snow that fell on the ice as well as true glacial ice values. Using the end-members of snow and GIS melt (Table 2) in an isotope mass balance, we determined that the contribution of snowmelt went from 100% during the first 2 weeks (early June) to 0–10% by the end of the fourth week of the snow melt season (late June to early July). This agrees with the field observations of when the majority of the periglacial snow cover had melted. After this, glacial melt and late June–August rain ($\delta^{18}O_{rain} = -16.9 \pm 4.7‰$, $n = 55$) contributed to river discharge. We note that this does not consider any potential fractionation that could result from evaporation, either in the river or on the glacier. In July, flow of Fox Canyon and other glacially sourced rivers was dominated by glacial melt (50–95% of discharge), which coincides with the peak season of GIS melt ("glacial melt"). As the season progressed, increased precipitation in the late summer contributed 5–25% to discharge ("mixed glacial/rain").

In contrast, the periglacial North Mountain River was fed by snow melt and rain. June discharge was dominated by snow melt, and July flow by spillover from the lake that forms the source of the river ("baseflow"). In late July through mid-August, flow was driven by the more frequent precipitation events.

3.2. Discharge and DOC Flux Dynamics

During the summers (June–August) of 2010–2012, the Fox Canyon and North Mountain Rivers discharged $0.6–1.3 \times 10^8$ and $0.3–1.1 \times 10^6$ m³ of water, respectively, and $4.5 \times 10^{-5}–8.2 \times 10^{-5}$ and $1.2 \times 10^{-6}–3.7 \times 10^{-6}$ Tg C/year as DOC. The greater DOC flux in Fox Canyon River was a result of its greater discharge. DOC concentrations in rivers running off the GIS were low but typical for concentrations reported for glacial runoff in other parts of Greenland (Bhatia et al., 2013; Lawson et al., 2014; Legrand et al., 2013) and elsewhere (Barker et al., 2006; Hood et al., 2015; Lafreniere & Sharp, 2004; Table 2).
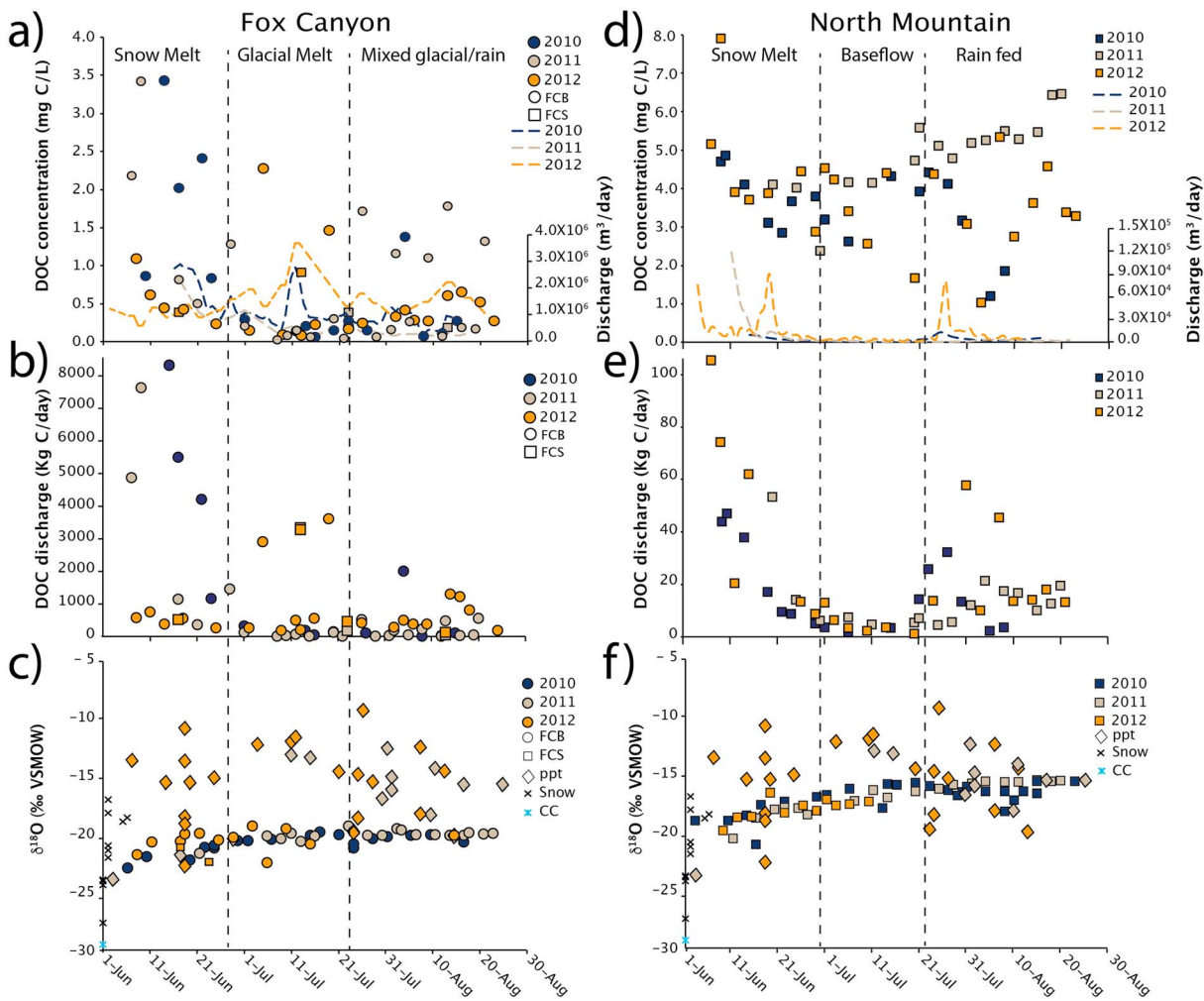
Figure 3. Time series of (a, d) dissolved organic carbon (DOC) concentrations and discharge, (b, e) DOC discharge, and (c, f) δ^{18}O (left) from Fox Canyon and (right) from North Mountain. Year 2010 is in blue, 2011 in gray, and 2012 in orange. (a) Squares represent samples from the source (FCS) and circles from the bridge (FCB). Note that Fox Canyon River has a higher discharge than North Mountain. Discharge measurements for Fox Canyon were made at the bridge (FCB), and the discharge curves (lines) represent a 2-point moving average of biweekly discharge measurements. (a–c) Circles represent samples taken at the bridge (FCB) squares at the source (FCS). Snow samples refer to samples taken from snow pits each May and any precipitation that fell as snow. Precipitation samples (ppt) represent rain (and sleet) and were collected in a bucket during each precipitation event. CC refers to a snow sample from a pit at Camp Century on the Greenland ice sheet. (d) Squares represent North Mountain DOC samples. Discharge curves were calculated by combining episodic discharge measurements with continuous measurements from a pressure transducer. (f) Squares represent samples from North Mountain; stream, ppt, snow, and CC are the same as those in panel (c).

Table 2
Mean Concentration and Range of DOC in Glacially and Nonglacially Sourced Rivers in NW Greenland Compared With Ranges From Central Greenland and Mountain Glaciers in Europe and Alaska

Region	Water source	Mean DOC (mg C/L)	DOC range (mg C/L)	DOC discharge (Tg C/year)	Reference
Thule (NW Greenland)	Glacial	0.67 ± 0.8	0.02–3.43	4.5×10^{-5}–8.2×10^{-5}	This study
Thule (NW Greenland)	Nonglacial	4.0 ± 1.3	1.02–6.46	1.2×10^{-6}–3.7×10^{-6}	This study
Central Greenland	Glacial	0.35 ± 0.4	0.06–1.49	5.2×10^{-4}–5.6×10^{-4}	Lawson et al. (2014)
Central Greenland	Glacial	0.58 ± 0.4	0.3–0.6	ND	Bhatia et al. (2013)
Central Greenland	Nonglacial (lake)	ND	0.4–7.4	ND	Bhatia et al. (2013)
Mountain glaciers	Glacial	ND	0.1–3.4	ND	Hood et al. (2015)

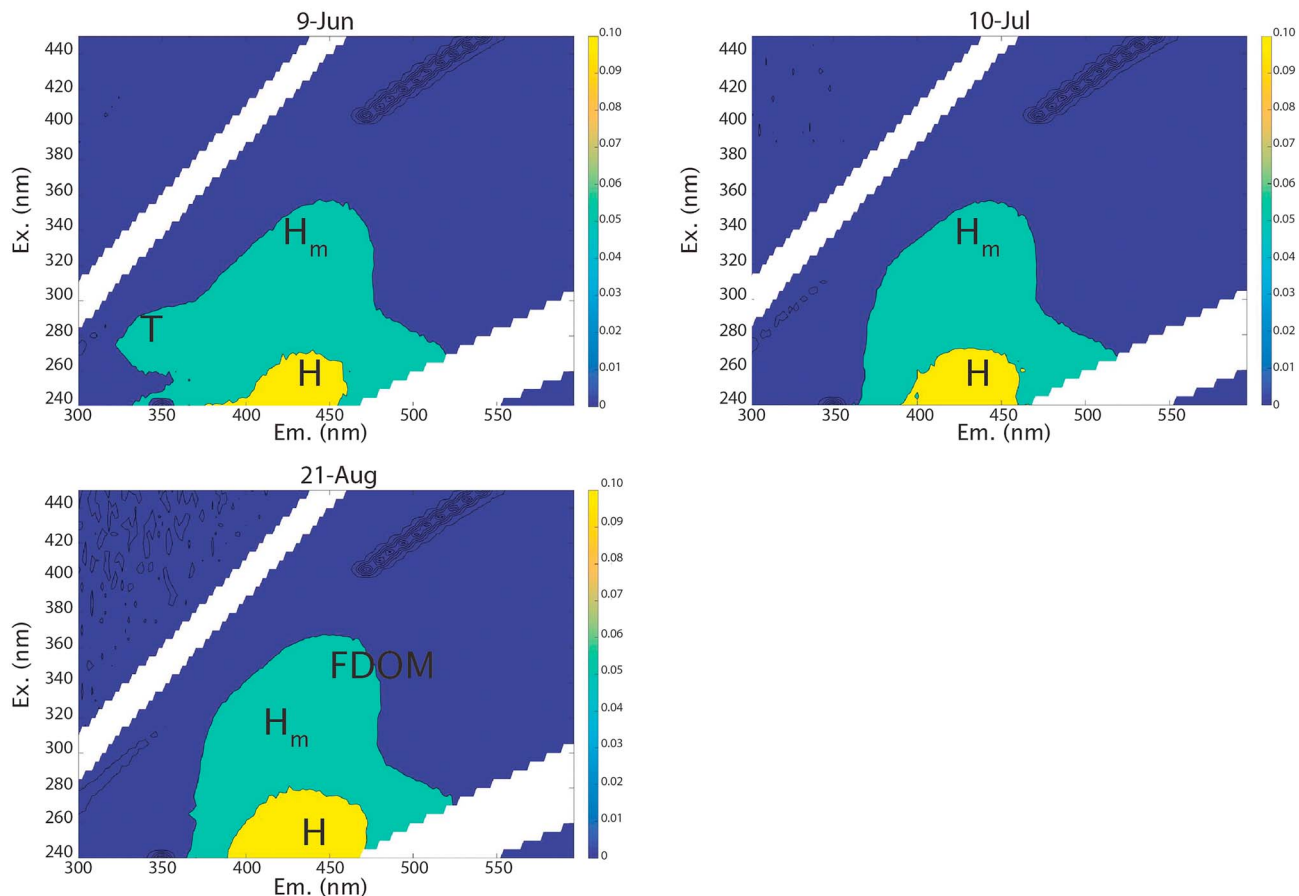*Note.* DOC = dissolved organic carbon; ND = no data.

Figure 4. Fluorescence excitation-emission matrices measured seasonally from North Mountain River. Humic-like peaks are indicated by an H. Hm indicates peaks that are humic like but representative of compounds that are common in soils (Coble, 2007). FDOM is an in situ peak that is highly correlated with dissolved organic carbon concentration (Spencer et al., 2007). T is the area of protein-like tryptophan peaks. Peaks are displayed in Ramen units.

DOC concentrations and discharge measured at the GIS-sourced Fox Canyon and periglacial North Mountain River were highest during the freshet and sharply decreased during the first 2 weeks after ice-off (Figure 3). The seasonal flux of DOC broadly followed the discharge curve with DOC concentrations at their highest during the spring freshet (Figures 3b and 3e). We also noted an increase in DOC concentrations in all rivers within a few days of episodic rain events, probably reflecting rapid drainage and C export from the surrounding sediments and soils. In 2011, DOC concentrations in the periglacial North Mountain River increased during the late summer. This was likely a consequence of lower precipitation and warmer temperatures in 2011 causing a reduction in lake level and thus streamflow promoting algal growth in the slower flowing water.

3.3. Composition of DOC

The fluorescence EEM spectra of DOC in our nonglacially sourced river was plant like (with humic-like EEM peaks: excitation 260 nm; emission 440 nm) throughout the entire summer (Figure 4).

In contrast, the composition of DOC exported by glacial rivers changed seasonally. The EEM spectra of DOC samples taken downstream in the glacially sourced Fox Canyon River (FCB) in June, were dominated by humic-like peaks, which when combined with the radiocarbon results (section 3.4) suggests that DOC during the freshet was likely derived from recently deposited plant matter or microbially produced young C (Figure 5). Later in the season (July–August), DOC became more microbially processed, as indicated by more protein-like EEM peaks (excitation 270; emission 340 nm; Figure 5). This late-season DOC was
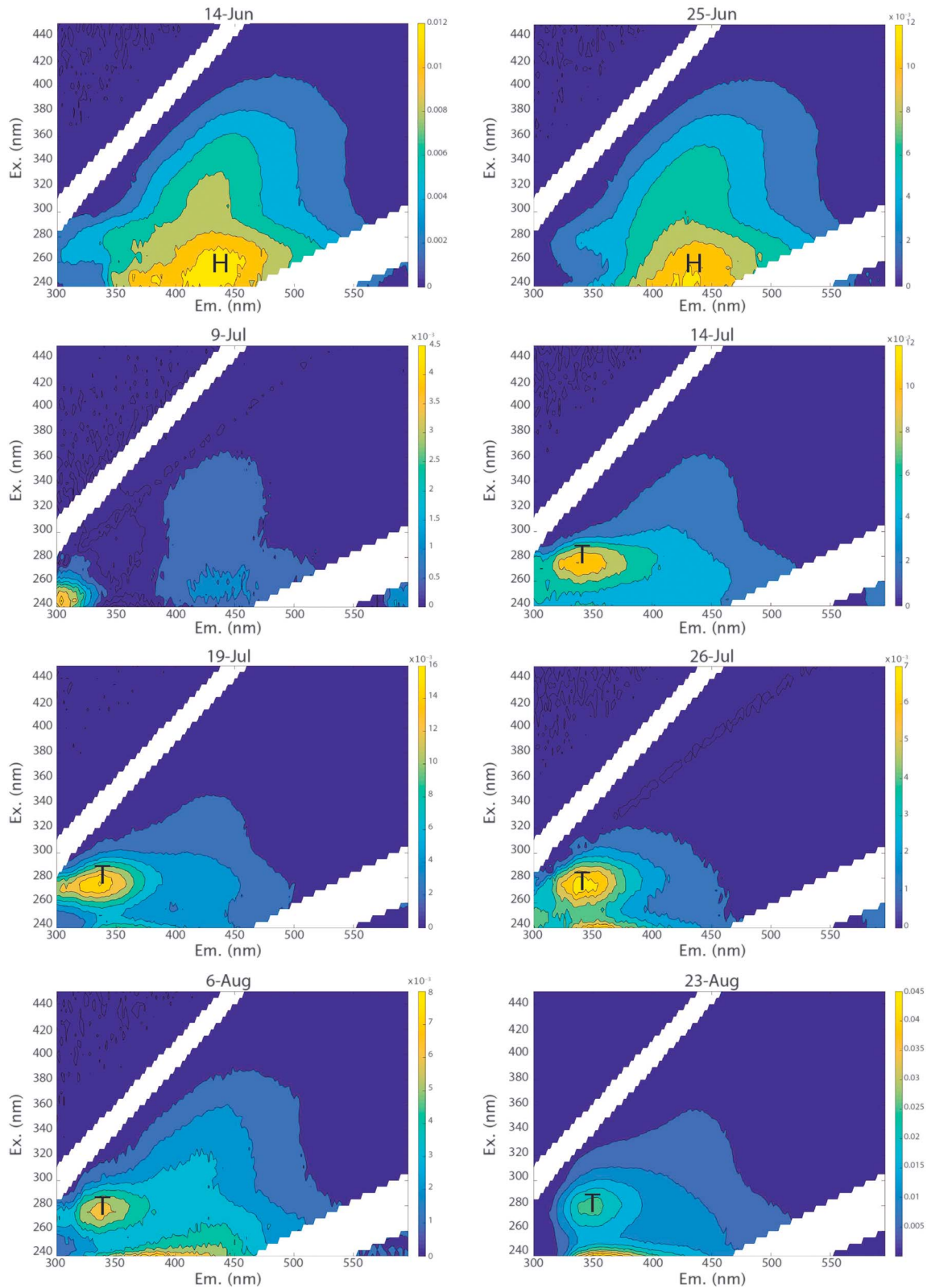
Figure 5. Fluorescence excitation-emission matrices from Fox Canyon River sampled downstream at the bridge. Humic-like peaks are indicated by an H, whereas tryptophan protein-like peaks are indicated by a T. Peaks are displayed in ramen units (RU).
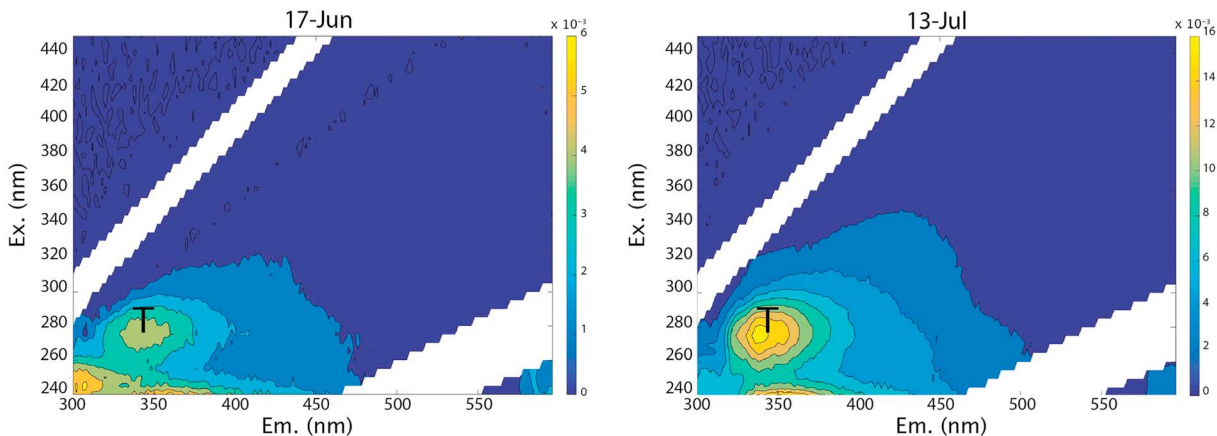
Figure 6. Fluorescence excitation-emission matrices measured in samples from Fox Canyon River taken at the Greenland ice sheet (GIS) source (FCS). T indicates tryptophan protein-like peaks. Peaks are displayed in Ramen units.

more similar to DOC sampled at the GIS (at the source of Fox Canyon River), which dominated by more processed autochthonous C with protein-like EEM signatures (Coble, 2007) throughout the season (Figure 6).

The seasonal transition from humic- to protein-like EEM peaks indicates that the periglacial landscape contributed the majority of the DOC during the early season and that glacial sources became more important as the season progressed.

Lawson et al. (2014) also found that protein-like peaks are common in glacially sourced rivers in midsummer, which may support the hypothesis of Bhatia et al. (2010) that ancient C exported from the GIS is microbially produced.

Earlier work by Bhatia et al. (2010) found that the composition of DOC in glacial outflow in Greenland also varied seasonally; however, in rivers with a subglacial flow component rivers varied from microbial (protein- and lipid-like) products dominating DOC during the early season to include a higher contribution of vascular plant-derived material during the late season. The results of Bhatia et al. from rivers with no subglacial flow show a similar seasonal pattern to ours.

Recent work suggests that DOC exported from glacial sources in summer is more bioavailable during transport than is DOC exported from nonglacial watersheds, because of lower rates of degradation and rapid transit times within the glacial environment (Hood et al., 2009; Lawson et al., 2014). Recently, Spencer et al. (2015) noted that ancient, permafrost-derived DOC in the Yukon Basin of interior Alaska is so labile that it is entirely consumed by the time the water reaches the river mouth. Given the rapid transit times (10–20 hr) in our study area, the majority of ancient DOC likely would complete the journey to the ocean to become an important component of the marine C cycle (Causey et al., 2014).

3.4. DOC and POC Ages

In all rivers, the average fraction modern value of DOC (F_{DOC}) was 0.8428 ± 0.0223 ($n = 39$; range 0.5947 to 1.0615), while the mean fraction modern of Northern Hemisphere atmospheric CO_2 (F_{air}) was 1.0465 in 2010, 1.0439 in 2011, and 1.0383 in 2012 (June to August at Point Barrow, AK, USA, $n = 3$–5 month^{-1}; X. Xu, personal communication, May 2016; Figure 7). Bulk riverine DOC represents a complex mixture of material, ranging in age from modern to old. However, $F_{DOC} < 1$ implies that the majority of DOC originated from older C pools that were fixed from atmospheric CO_2 before 1950 (prior to thermonuclear weapon's testing; Schuur et al., 2016). These older C pools may include aged (^{14}C depleted, e.g., organic matter in mineral soils) and fossil (^{14}C free, e.g., shale) deposits and their microbial degradation products. In contrast, $F_{DOC} > F_{air}$ indicates that the majority of the DOC originated from "modern" C (fixed from atmospheric CO_2 during the post-bomb era).
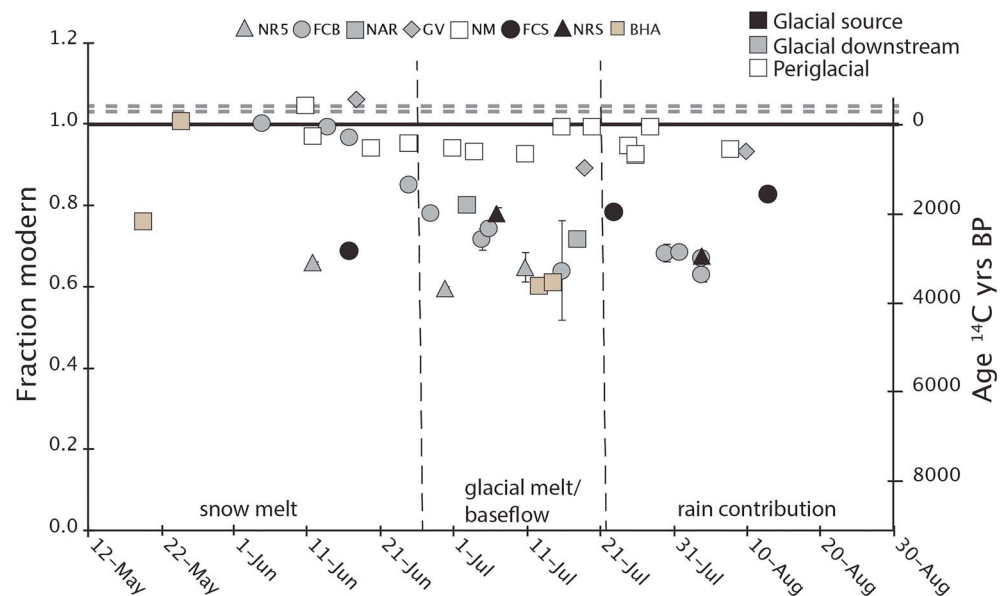
Figure 7. Seasonal time series of radiocarbon (in fraction modern [F]) of dissolved organic carbon from all study years (2010–2012) and all sites including four glacially sourced (filled symbols) and one periglacial (open symbols) river. Tan symbols are from radiocarbon measurements made in glacially sourced rivers in central Greenland by Bhatia et al. (2013). Solid horizontal line indicates $F = 1$ (0 years BP, which is 1950). Dashed horizontal lines indicate the range of F in background atmospheric CO_2 during June to August 2010 to 2012 (Point Barrow, AK, USA; Xu, personal communication, 2016).

We observed the most ^{14}C-enriched DOC is in the periglacial river (North Mountain, $F = 0.9233$–1.0479) and the glacially sourced Green Valley River ($F = 0.8919$–1.0615). These rivers drain more productive watersheds than do the other rivers; hence, their DOC has a larger contribution of recently fixed plant C. It is also possible that the source of young C in these rivers may be contributed by microbes living in glacial forefields (Bradley et al., 2014).

There are very few studies with which we can compare our data; however, DO[14]C data exist for glacial runoff from further south in Greenland and in the Gulf of Alaska. Radiocarbon values for DOC exported in the Fox Canyon ($F = 0.6291$–1.0022, $n = 15$), North ($F = 0.5947$–0.7813, $n = 5$), and Narssarssuk Rivers ($F = 0.7176$–0.8024, $n = 2$) were (except during the freshet) much more depleted than those measured in large Arctic rivers ($F = 0.8919$–1.1334, $n = 60$; Raymond et al., 2007) but similar to that reported for glacial runoff in southeast Alaska ($F = 0.6183$; Hood et al., 2009) and central Greenland ($F = 0.6033$–0.7594, $n = 14$; Bhatia et al., 2013).

For the two rivers with the longest observation period (Fox Canyon and North Mountain) as well as Green Valley, our data also showed a clear seasonal trend toward older (more ^{14}C depleted) DOC ages as the summer progresses (Figure 7). This seasonal trend is consistent with observations by Bhatia et al. (2013) in central Greenland.

Stubbins et al. (2012) postulated that the majority of ancient (^{14}C-depleted) DOC in glacial outflow may be sourced directly from glacial ice and consists of carbonaceous aerosol derived from fossil fuel combustion. However, Bhatia et al. (2013) noted that in central Greenland, DOC in supraglacial lakes in July was more ^{14}C enriched ($F = 0.7661 \pm 0.0231$, $n = 2$) than DOC in glacial outflow ($F = 0.6062 \pm 0.0029$, $n = 2$). They concluded that the seasonal depletion of glacial outflow DO[14]C was related to the seasonal evolution of a subglacial drainage system and that the source of the ^{14}C-depleted DOC were ancient, subglacial C pools from time periods when the GIS was inland from its present position.

In our study area, evidence of subglacial flow has only been clearly shown for North River (Cameron et al., 2015). More importantly, it is unlikely that the glacial Narssarssuk River, which drains a very small glacier disconnected from the GIS, or the periglacial North Mountain River, also disconnected from the GIS, drain
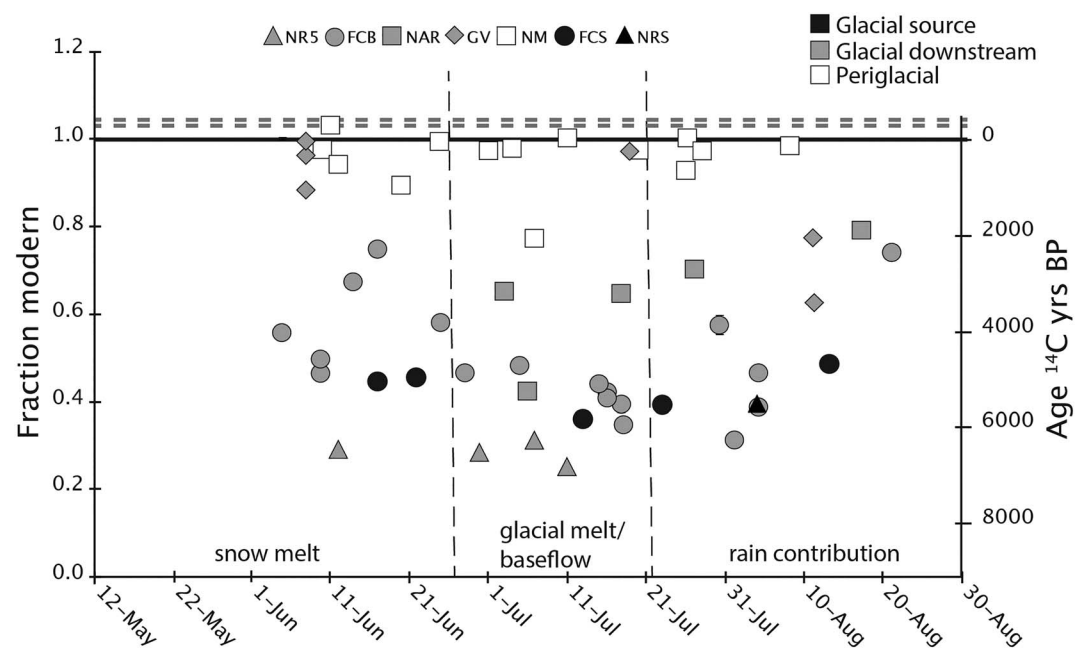
Figure 8. Time series of radiocarbon (in fraction modern [F]) of particulate organic carbon in (full symbols) four glacially sourced and (open square) one periglacial river in NW Greenland. For glacially sourced rivers, black symbols indicate sampling sites near the source and gray symbols sampling downstream. Solid horizontal line indicates $F = 1$ (0 years BP). Dashed horizontal lines indicate the range of F in background atmospheric CO_2 during June to August 2010 to 2012 (Point Barrow, AK, USA; Xu, personal communication, 2016).

large subglacial C pools or receive large inputs of fossil carbonaceous aerosol. Therefore, the predominance of ^{14}C-depleted DOC in our study region strongly suggests that all rivers are exporting C that originates from aged C stored in permafrost in the glacier foreland (Czimczik & Welker, 2010; Hågvar & Ohlson, 2013; Horwath et al., 2008; Lupascu, Welker, Seibt, Xu, et al., 2014), in addition to any subglacial and englacial C fluxes (Bhatia et al., 2013). The relative contribution of this permafrost soil C to the DOC export is likely greatest in August when the active layer is deepest and cooling temperatures have reduced the amount of discharge from the GIS.

The ice margin in the Thule area has changed substantially over the past several million years with multiple advances and retreats of the GIS during glacial-interglacial cycles over that time period (e.g., Alley et al., 2010; Masson-Delmotte et al., 2012). Regional studies (e.g., Bennike & Böcher, 1992; Hedenäs & Bennike, 2003) noted the presence of abundant interglacial deposits in the Thule area dating to 115,000–130,000 years BP. Any organic matter contributed from the last interglacial period would be ^{14}C-dead ($F = 0$). Further, Horwath et al. (2008) identified old C-rich soil layers buried in the Fox Canyon catchment ($F = 0.0189$ to 0.0327). These deposits are located within the active layer and may be eroded by subsurface runoff along the permafrost boundary. Such deposits may continue underneath the GIS and may be a possible source of ancient C exported from subglacial streamflow. Measurements of permafrost C contributing to the aqueous portions of the C cycle in combination with measurements of permafrost C contributing to gaseous C emissions in NW Greenland (Czimczik & Welker, 2010; Lupascu et al., 2014; Lupascu, Welker, Seibt, Xu, et al., 2014) reinforce the postulate that ancient permafrost C is becoming a more important component of DOC flux in NW Greenland and the Arctic.

Mean PO[14]C values (Figure 8) were on average more depleted (F = 0.6455 ± 0.0344, $n = 55$; range 0.2506 to 1.0366) than DO[14]C values. This suggests that POC is primarily derived from the physical erosion of aged C pools, while DOC is a mixture of aged and recent C sources. Similar to DO[14]C, we observed the most ^{14}C-enriched POC was in the periglacial North Mountain ($F = 0.7753$–1.0366) and glacial Green Valley (0.6276–0.9937) Rivers that drain more productive watersheds. As with DO[14]C, PO[14]C became more depleted as the summer progressed in all rivers. In Fox Canyon River ($F = 0.3140$–0.7503) the most depleted PO[14]C values occurred in mid-July at the same time as peak discharge, suggesting that the source of much of
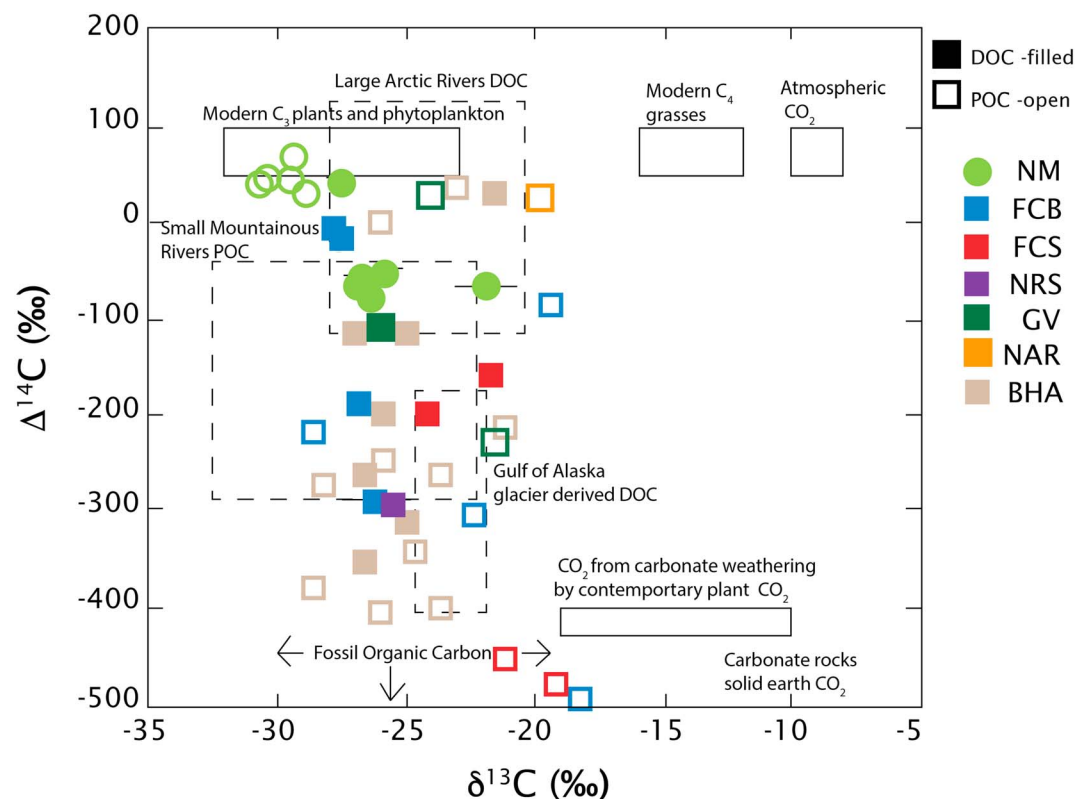
Figure 9. Dissolved and particulate organic $\Delta^{14}C$ and $\delta^{13}C$ in glacially sourced and nonglacially sourced water samples collected near Thule Air Force Base, Greenland. This figure has been modified from Bhatia et al. (2013), where solid boxes illustrate isotopic ranges of end-member carbon sources (Mayorga et al., 2005), dashed boxes illustrate literature values for large Arctic rivers dissolved organic carbon (DOC; Raymond et al., 2007), small mountainous rivers particulate organic carbon (POC; Raymond & Bauer, 2001), and Gulf of Alaska glacially derived DOC (Hood et al., 2009). The fossil organic carbon source is radiocarbon dead ($\Delta^{14}C = -1,000‰$) and can have $\delta^{13}C$ values ranging from $-15‰$ to $-35‰$. Values measured by Bhatia et al. (2013) from rivers in western Greenland are depicted in light brown and denoted as BHA.

the ancient POC may be derived from river bank erosion. In contrast to $DO^{14}C$, we observed interannual differences in $PO^{14}C$, but only in the periglacial North Mountain River. Here $PO^{14}C$ was more enriched in 2011 ($F = 1.0043 \pm 0.0076$, $n = 6$) than in 2010 or 2012 ($F = 0.9115 \pm 0.0681$ or 0.99465 ± 0.0158, $n = 3$ or 5, respectively). We attribute this to an increase in algal growth as North Mountain River became stagnant during the dry and warm year 2011.

3.5. GIS Versus Landscape C Contributions

At Fox Canyon River, the amount of DOC contributed from each source varied seasonally. Landscape C export was the dominant DOC source during the freshet, while the GIS was the dominant DOC source throughout the remainder of the summer. In late summer, however, episodic rain events decreased the GIS contribution to ~50%. It should also be noted that the majority of total C exported from glacially sourced rivers (60–70%) was exported during the first 2 weeks after freshet.

A plot of the $\delta^{13}C$ and $\Delta^{14}C$ values of DOC and POC measured in our western Greenland rivers are presented in Figure 9. $\delta^{13}C$ values of DOC range from $-21.7‰$ to $-27.7‰$, whereas the $\delta^{13}C$ values of POC have a much large range of $-15.2‰$ to $-30.4‰$. POC $\delta^{13}C$ and $\Delta^{14}C$ values from the nonglacially sourced river North Mountain plot almost entirely within the range that would be expected for modern C_3 vegetation and phytoplankton, suggesting that the POC in this river is primarily derived from modern vegetation with little contribution of recalcitrant ancient POC from the soil (Figure 9). North Mountain $\Delta^{14}C_{DOC}$ by contrast, apart from measurements made during freshet, is much more depleted, suggesting that DOC exported to this river is derived from older C pools, most likely relict soil C stored in the active layer. In glacially sourced

rivers POC δ^{13}C values become more enriched as the season progresses, suggesting an increasing contribution from recalcitrant sources late in the season. In the plot of δ^{13}C and Δ^{14}C presented in Figure 9 glacially sourced rivers (e.g., FCB) have values that fall within the same range as those measured by Bhatia et al. (2013).

3.6. DOC Fluxes From the GIS and Surrounding Landscape

If the DOC fluxes observed in individual catchments are extrapolated to the entire GIS, then flux estimates from the GIS range from 0.08 to 0.22 Tg C/year (Bhatia et al., 2013; Hood et al., 2015; Lawson et al., 2014). Using the similar methods described in these earlier studies, we obtained modeled annual runoff from the GIS from the MAR (Modèle Atmosphérique Régional) regional climate model. We then used our average DOC concentrations for Fox Canyon River, weighted by discharge, to scale our DOC fluxes to the entire GIS—assuming that our catchments represent the range of watershed types in Greenland.

In order to scale our flux estimates, we calculated monthly averages of DOC weighted by discharge. Because we only had discharge measurements from North Mountain and Fox Canyon, we could not produce discharge weighted means from other watersheds. However, seasonal DOC concentrations were similar in all glacially sourced rivers; therefore, we can assume that Fox Canyon is representative of an average glacially sourced river. We obtained discharge weighted means for Fox Canyon River of 0.91 (2010), 1.03 (2011), and 0.53 mg C/L (2012). The discharge weighted mean was determined by weighting the DOC concentration by discharge at the time of measurement and then averaging the DOC concentration over each month, multiplied by the number of days in that month and summed to arrive at a 3-month summer flux. Because no discharge was observed in winter, this 3-month flux is a good approximation of the annual flux in each year. The main reason for the much lower average DOC concentration in 2012 is likely that the river started flowing earlier that year (in late May), and we were unable to begin measuring immediately upon breakup. We typically observed the highest DOC concentrations during the 2 weeks immediately following breakup (Figure 3).

Next, we obtained modeled estimates of annual runoff from the GIS from the MAR regional climate model (Fettweis et al., 2011, 2017; Tedesco et al., 2013). The MAR model uses reanalysis data to model runoff, and we used the runoff values estimated by the National Centers for Environmental Prediction/National Center for Atmospheric Research (NCEP/NCAR) reanalysis. These values were 499 (2010), 371 (2011), and 541 km^3/year (2012; Fettweis et al., 2017). We also used the average GIS runoff for the 1961–1990 period (251 $\pm$ 50 km^3/year).

Using modeled annual runoff, we obtained estimates of riverine DOC export from the GIS of 0.29% to 0.45% $\pm$ 20% Tg C/year for 2010–2012. Our estimates are higher than previous estimates made by scaling riverine DOC concentrations—0.08 $\pm$ 0.02 Tg C/year (Bhatia et al., 2013) and 0.13% to 0.17% $\pm$ 13% Tg C/year (Lawson et al., 2014)—and higher than recent estimates made by scaling DOC concentrations taken directly from the surface of the GIS of 0.22 $\pm$ 0.02 Tg C/year (Hood et al., 2015). We should note that our measurements contain much higher DOC concentrations in the early season (first 2 weeks of freshet) than either previous study, most likely because our downstream sampling site (Fox Canyon bridge) was located further downstream than either of the localities sampled in the Bhatia et al. (2013) or Lawson et al. (2014) study. Our study period also encompasses two of the highest melt years on the GIS (2010 and 2012), with associated high glacial runoff (Tedesco et al., 2013). If instead of using modeled runoff values for the specific years of our study we use the average GIS runoff for the period 1961–1990 (251 $\pm$ 50 km^3/year) used by Bhatia et al. (2013), we obtain smaller estimates of 0.13–0.26 Tg C/year, which are closer to the estimates obtained by Lawson et al. (2014). If we only look at the average DOC concentrations post freshet, our DOC concentrations are comparable with prior studies, and using these averages and the average GIS runoff from 1961 to 1990, we obtain estimates of GIS DOC flux of 0.09% to 0.16% $\pm$ 20% Tg C/year, matching those obtained by prior studies. These discrepancies in GIS annual DOC flux estimates indicate that in order to accurately represent the annual flux of C from the GIS, it is extremely important to sample a wide variety of river catchments, to sample downstream as well as near the source, and to begin sampling as soon as rivers start to flow. Finally, our flux results indicate that the highest C fluxes occur during the time of year when the majority of C is modern in age. However, although warmer temperatures could result in increased young C through enhanced plant growth, higher melt rates from the GIS and greater permafrost thaw could result in increasing amounts of ancient C from the GIS and from the periglacial landscape to the ocean.

4. Conclusions

Our study demonstrates the complexity of watersheds and interannual and seasonal variation in runoff and DOC export in Greenland. During the summer (June, July, and August), rivers (both glacial and nonglacial) in the Thule peninsula of NW Greenland transfer $4.6–8.6 \times 10^{-5}$ Tg of terrestrial C to the coastal ocean as DOC. Most of the annual DOC (60–76%) is exported during the freshet by GIS-sourced rivers and consists of relatively young ($F = 0.9667–1.0022 \pm 0.0024$ (1σ)), microbially processed C derived from soils and sediments in the glacier foreland. Scaled to the GIS, we estimate a flux of 0.29–0.45% $\pm$ 20% Tg DOC/year (2010–2012).

Glacial melt and summer precipitation events contribute 20–30% to the total annual DOC flux and export older DOC ($F = 0.6291–0.7450 \pm 0.0218$). Up to 30% of this aged DOC is derived from periglacial C sources. Ongoing climate warming (permafrost thaw) and wetting are likely to increase the transfer of periglacial permafrost C to the coastal ocean. Our study also suggests that future DOC flux estimates need to consider increasing Arctic plant productivity, since we found highly concentrated, young ($F = 0.8919–1.0615 \pm 0.0023$) DOC in a GIS-sourced river draining our most productive watershed. We also would like to note that future studies of total C flux from the GIS should consider adopting a common seasonal sampling period, including the initial freshet, from a larger number of rivers and positions along the rivers to more accurately determine the total C flux.

References

Alley, R. B., Andrews, J. T., Brigham-Grette, J., Clarke, G. K. C., Cuffey, K. M., Fitzpatrick, J. J., et al. (2010). History of the Greenland ice sheet: Paleoclimatic insights. *Quaternary Science Reviews*, *29*(15-16), 1728–1756. https://doi.org/10.1016/j.quascirev.2010.02.007

Amon, R. M. W. (2004). The role of dissolved organic matter for the organic carbon cycle in the Arctic Ocean. In R. S. Stein & R. W. Macdonald (Eds.), *The organic carbon cycle in the Arctic Ocean* (pp. 83–99). New York: Springer.

Bamber, J., van den Broeke, M., Ettema, J., Lenaerts, J., & Rignot, E. (2012). Recent large increases in freshwater fluxes from Greenland into the North Atlantic. *Geophysical. Research Letters*, *39*, L19501. https://doi.org/10.1029/2012GL052552

Barker, J. D., Sharp, M. J., Fitzsimons, S. J., & Turner, R. J. (2006). Abundance and dynamics of dissolved organic carbon in glacier systems. *Arctic, Antarctic, and Alpine Research*, *38*(2), 163–172. https://doi.org/10.1657/1523-0430(2006)38[163:AADODO]2.0.CO;2

Benner, R., Louchouarn, P., & Amon, R. M. W. (2005). Terrigenous dissolved organic matter in the Arctic Ocean and its transport to surface and deep waters of the North Atlantic. *Global Biogeochemical Cycles*, *19*, GB2025. https://doi.org/10.1029/2004GB002398

Bennike, O., & Böcher, J. (1992). Early Weichselian interstadial land biotas at Thule, northwest Greenland. *Boreas*, *21*, 111–118.

Beverly, R. K., Beaumont, W., Tauz, D., Ormsby, K. M., von Reden, K. F., Santos, G. M., & Southon, J. R. (2010). The Keck Carbon AMS Laboratory, University of California, Irvine: Status report. *Radiocarbon*, *52*(02), 301–309. https://doi.org/10.1017/S0033822200045343

Bhatia, M. P., Das, S. B., Kujawinski, E. B., Henderson, P., Burke, A., & Charette, M. A. (2011). Seasonal evolution of water contributions to discharge from a Greenland outlet glacier: Insight from a new isotope-mixing model. *Journal of Glaciology*, *57*(205), 929–941. https://doi.org/10.3189/002214311798043861

Bhatia, M. P., Das, S. B., Longnecker, K., Charette, M. A., & Kujawinski, E. B. (2010). Molecular characterization of dissolved organic matter associated with the Greenland ice sheet. *Geochimica et Cosmochimica Acta*, *74*(13), 3768–3784. https://doi.org/10.1016/j.gca.2010.03.035

Bhatia, M. P., Das, S. B., Xu, L., Charette, M. A., Wadham, J. L., & Kujawinski, E. B. (2013). Organic carbon export from the Greenland ice sheet. *Geochimica et Cosmochimica Acta*, *109*, 329–344. https://doi.org/10.1016/j.gca.2013.02.006

Bintanja, R., & Selten, F. M. (2014). Future increases in Arctic precipitation linked to local evaporation and sea-ice retreat. *Nature*, *509*(7501), 479–482. https://doi.org/10.1038/nature13259

Blanc-Betes, E., Welker, J. M., Sturchio, N. C., Chanton, J. P., & Gonzalez-Meler, M. A. (2016). Winter precipitation and snow accumulation drive the methane sink or source strength of Arctic tussock tundra. *Global Change Biology*, *22*(8), 2818–2833. https://doi.org/10.1111/gcb.13242

Bradley, J. A., Singarayer, J. S., & Anesio, A. M. (2014). Microbial community dynamics in the forefield of glaciers. *Proceedings of the Royal Society B*, *281*(1795). https://doi.org/10.1098/rspb.2014.0882

Burnham, J. H., & Sletten, R. S. (2010). Spatial distribution of soil organic carbon in northwest Greenland and underestimates of high Arctic carbon stores. *Global Biogeochemical Cycles*, *24*, GB3012. https://doi.org/10.1029/2009GB003660

Cameron, K. A., Hagedorn, B., Dieser, M., Christner, B. C., Choquette, K., Sletten, R., et al. (2015). Diversity and potential sources of microbiota associated with snow on western portions of the Greenland ice sheet. *Environmental Microbiology*, *17*(3), 594–609. https://doi.org/10.1111/1462-2920.12446

Causey, D., Welker, J. M., Burnham, K. K., Padula, V. M., & Bargmann, N. A. (2014). Fine-scale temporal and spatial patterns of a high Arctic marine bird community. In F. J. Mueter, D. M. S. Dickson, H. P. Huntington, J. R. Irvine, E. A. Logerwell, S. A. MacLean, L. T. Quakenbush, & C. Rosa (Eds.), *Responses of Arctic marine ecosystems to climate change* (pp. 171–189). Alaska Sea Grant: University of Alaska Fairbanks.

Clausen, H. B., Gundestrup, N. S., Johnsen, S. J., Bindschadler, R., & Zwally, J. (1988). Glaciological investigations in the Crete area, central Greenland: A search for a new deep-drilling site. *Annals of Glaciology*, *10* International Glaciological Society, 10–15. https://doi.org/10.1017/S0260305500004080

Coble, P. G. (1996). Characterization of marine and terrestrial DOM in seawater using excitation-emission matrix spectroscopy. *Marine Chemistry*, *51*(4), 325–346. https://doi.org/10.1016/0304-4203(95)00062-3

Coble, P. G. (2007). Marine optical biogeochemistry: The chemistry of ocean color. *Chemical Reviews*, *107*(2), 402–418. https://doi.org/10.1021/cr050350+

Commane, R., Lindaas, J., Benmergui, J., Luus, K. A., Chang, R. Y.-W., Daube, B. C., et al. (2017). Carbon dioxide sources from Alaska driven by increasing early winter respiration from Arctic tundra. *PNAS*, *114*(21), 5361–5366. https://doi.org/10.1073/pnas.1618567114

Czimczik, C. I., & Welker, J. M. (2010). Radiocarbon content of CO_2 respired from high Arctic tundra in northwest Greenland. *Arctic, Antarctic and Alpine Research*, *42*(3), 342–350. https://doi.org/10.1657/1938-4246-42.3.342

Dansgaard, W., Johnsen, S. J., Moller, J., & Langway, C. C. (1969). One thousand centuries of climatic record from Camp Century on the Greenland ice sheet. *Science*, *166*(3903), 377–380. https://doi.org/10.1126/science.166.3903.377

Elmendorf, S. C., Henry, G. H. R., Hollister, R. D., Björk, R. G., Bjorkman, A. D., Callaghan, T. V., et al. (2012). Global assessment of experimental climate warming on tundra vegetation: Heterogeneity over space and time. *Ecology Letters*, *15*(2), 164–175. https://doi.org/10.1111/j.1461-0248.2011.01716.x

Fellman, J. B., D'Amore, D. V., Hood, E., & Boone, R. D. (2008). Fluorescence characteristics and biodegradability of dissolved organic matter in forest and wetland soils from coastal temperate watersheds in southeast Alaska. *Biogeochemistry*, *88*(2), 169–184. https://doi.org/10.1007/s10533-008-9203-x

Fellman, J. B., Hood, E., & Spencer, R. G. M. (2010). Fluorescence spectroscopy opens new windows into dissolved organic matter dynamics in freshwater ecosystems: A review. *Limnology and Oceanography*, *55*(6), 2452–2462. https://doi.org/10.4319/lo.2010.55.6.2452

Fettweis, X., Box, J. E., Agosta, C., Amory, C., Kittel, C., Lang, C., et al. (2017). Reconstructions of the 1900–2015 Greenland ice sheet surface mass balance using the regional climate MAR model. *The Cryosphere*, *11*, 1015–1033. https://doi.org/10.5194/tc-11-1015-2017

Fettweis, X., Tedesco, M., van den Broeke, M., & Ettema, J. (2011). Melting trends over the Greenland ice sheet (1958–2009) from space-borne microwave data and regional climate models. *The Cryosphere*, *5*, 359–375. https://doi.org/10.5194/tc-5-359-2011

Hågvar, S., & Ohlson, M. (2013). Ancient carbon from a melting glacier gives high ^{14}C age in living pioneer invertebrates. *Scientific Reports*, *3*(1). https://doi.org/10.1038/srep02820

Hanna, E., Mernild, S. H., Cappelen, J., & Steffen, K. (2012). Recent warming in Greenland in a long-term instrumental (1881–2012) climatic context: I. Evaluation of surface air temperature records. *Environmental Research Letters*, *7*(4). https://doi.org/10.1088/1748-9326/7/4/045404

Hedenäs, L., & Bennike, O. (2003). Moss remains from the last interglacial at Thule, NW Greenland. *Lindbergia*, *28*, 52–58.

Hilton, R. G., Galy, V., Gaillardet, J., Dellinger, M., Bryant, C., O'Regan, M., et al. (2015). Erosion of organic carbon in the Arctic as a geological carbon dioxide sink. *Nature*, *524*(7563), 84–87. https://doi.org/10.1038/nature14653

Hood, E., Battin, T. J., Fellman, J., O'Neel, S., & Spencer, R. G. M. (2015). Storage and release of organic carbon from glaciers and ice sheets. *Nature Geoscience*, *8*(2), 91–96. https://doi.org/10.1038/ngeo2331

Hood, E., Fellman, J., Spencer, R. G. M., Hernes, P. J., Edwards, R., D'Amore, D., & Scott, D. (2009). Glaciers as a source of ancient and labile organic matter to the marine environment. *Nature*, *462*, 1044–1047. https://doi.org/10.1038/nature08580

Horwath, J. L., Sletten, R. S., Hagedorn, B., & Hallet, B. (2008). Spatial and temporal distribution of soil organic carbon in nonsorted striped patterned ground of the high Arctic. *Journal of Geophysical Research*, *113*, G03S07. https://doi.org/10.1029/2007JG000511

Hugelius, G., Strauss, J., Zubrzycki, S., Harden, J. W., Schuur, E. A. G., Ping, C.-L., et al. (2014). Estimated stocks of circumpolar permafrost carbon with quantified uncertainty ranges and identified data gaps. *Biogeosciences*, *11*(23), 6573–6593. https://doi.org/10.5194/bg-11-6573-2014

Kicklighter, D. W., Hayes, D. H., McClelland, J. W., Peterson, B. J., McGuire, A. D., & Melillo, J. M. (2013). Insights and issues with simulating terrestrial DOC loading of Arctic river networks. *Ecological Applications*, *23*, 1817–1836. https://doi.org/10.1890/11-1050.1

Lafreniere, M. J., & Sharp, M. J. (2004). The concentration and fluorescence of dissolved organic carbon (DOC) in glacial and nonglacial catchments: Interpreting hydrological flow routing and DOC sources. *Arctic, Antarctic and Alpine Research*, *36*(2), 156–165. https://doi.org/10.1657/1523-0430(2004)036[0156:TCAFOD]2.0.CO;2

Lawson, E. C., Wadham, J. L., Tranter, M., Stibal, M., Lis, G. P., Butler, C. E. H., et al. (2014). Greenland ice sheet exports labile organic carbon to the Arctic oceans. *Biogeosciences*, *11*, 4015–4028. https://doi.org/10.5194/bg-11-4015-2014

Legrand, M., Preunkert, S., Jourdain, B., Guilhermet, J., Faïn, X., Alekhina, I., & Petit, J. R. (2013). Water-soluble organic carbon in snow and ice deposited at Alpine, Greenland and Antarctic sites: A critical review of available data and their atmospheric relevance. *Climate of the Past*, *9*, 2195–2211. https://doi.org/10.5194/cp-9-2195-2013

Lupascu, M., Welker, J. M., Seibt, U., Maseyk, K., Xu, X., & Czimczik, C. I. (2014). High Arctic wetting reduces permafrost carbon feedbacks to climate warming. *Nature Climate Change*, *4*(1), 51–55. https://doi.org/10.1038/nclimate2058

Lupascu, M., Welker, J. M., Seibt, U., Xu, X., Velicogna, I., Lindsey, D. S., & Czimczik, C. I. (2014). The amount and timing of precipitation control the magnitude, seasonality and sources (^{14}C) of ecosystem respiration in a polar semi-desert, northwestern Greenland. *Biogeosciences*, *11*, 4289–4304. https://doi.org/10.5194/bg-11-4289-2014

Masson-Delmotte, V., Swingedouw, D., Landais, A., Seidenkrantz, M. S., Gauthier, E., Bichet, V., et al. (2012). Greenland climate change: From the past to the future. *WIREs Climate Change*, *3*(5), 427–449. https://doi.org/10.1002/wcc.186

Mayorga, E., Aufdenkampe, A. K., Masiello, C. A., Krusche, A. V., Hedges, J. I., Quay, P. D., et al. (2005). Young organic matter as a source of carbon dioxide outgassing from Amazonian rivers. *Nature*, *436*(7050), 538–541. https://doi.org/10.1038/nature03880

McClelland, J. W., Holmes, R. M., Dunton, K. H., & Macdonald, R. W. (2012). The Arctic Ocean estuary. *Estuaries and Coasts*, *35*(2), 353–368. https://doi.org/10.1007/s12237-010-9357-3

McConnell, J. R., Edwards, R., Kok, G. L., Flanner, M. G., Zender, C. S., Saltzman, E. S., et al. (2007). 20th-century industrial black carbon emissions altered Arctic climate forcing. *Science*, *317*(5843), 1381–1384. https://doi.org/10.1126/science.1144856

Mote, T. L. (2007). Greenland surface melt trends 1973–2007: Evidence of a large increase in 2007. *Geophysical Research Letters*, *34*, L22507. https://doi.org/10.1029/2007GL031976

Mouteva, G. O., Fahrni, S. M., Sanots, G. M., Randerson, J. T., Zhang, Y.-L., Szidat, S., & Czimczik, C. I. (2015). Accuracy and precision of ^{14}C-based source apportionment of organic and elemental carbon in aerosols using the Swiss_4S protocol. *Atmospheric Measurement Techniques*, *8*(9), 3729–3743. https://doi.org/10.5194/amt-8-3729-2015

Neff, J. C., Finlay, J. C., Zimov, S. A., Davydov, S. P., Carrasco, J. J., Schuur, E. A. G., & Davydova, A. I. (2006). Seasonal changes in the age and structure of dissolved organic carbon in Siberian rivers and streams. *Geophysical Research Letters*, *33*, L23401. https://doi.org/10.1029/2006GL028222

Nghiem, S. V., Hall, D. K., Mote, T., Tedesco, M., Albert, M. R., Keegan, K., et al. (2012). The extreme melt across the Greenland ice sheet in 2012. *Geophysical Research Letters*, *39*, L18502. https://doi.org/10.1029/2012GL053611

Raymond, P. A., & Bauer, J. E. (2001). Riverine export of aged terrestrial organic matter to the North Atlantic Ocean. *Nature*, *409*(6819), 497–500. https://doi.org/10.1038/35054034

Raymond, P. A., McClelland, J. W., Holmes, R. M., Zhulidov, A. V., Mull, K., Peterson, B. J., et al. (2007). Flux and age of dissolved organic carbon exported to the Arctic Ocean: A carbon isotopic study of the five largest Arctic rivers. *Global Biogeochemical Cycles*, *21*, GB4011. https://doi.org/10.1029/2007GB002934

Rignot, E., Box, J. E., Burgess, E., & Hanna, E. (2008). Mass balance of the Greenland ice sheet from 1958 to 2007. *Geophysical Research Letters*, *35*, L20502. https://doi.org/10.1029/2008GL035417

Rignot, E., Koppes, M., & Velicogna, I. (2010). Rapid submarine melting of the calving faces of west Greenland glaciers. *Nature Geoscience*, *3*(3), 187–191. https://doi.org/10.1038/ngeo765

Romanovsky, V. E., Smith, S. L., & Christiansen, H. H. (2010). Permafrost thermal state in the polar Northern Hemisphere during the international polar year 2007–2009: A synthesis. *Permafrost and Periglacial Processes*, *21*(2), 106–116. https://doi.org/10.1002/ppp.689

Schuur, E. A., Druffel, E., & Trumbore, S. E. (2016). *Radiocarbon and climate change: Mechanisms, applications and laboratory techniques*. New York: Springer. https://doi.org/10.1007/978-3-319-25643-6_3

Serreze, M. C., & Barry, R. G. (2011). Processes and impacts of Arctic amplification: A research synthesis. *Global and Planetary Change*, *77*, 85–96. https://doi.org/10.1016/j.gloplacha.2011.03.004

Sharp, E., Sullivan, P., Steltzer, H., Csank, A. Z., & Welker, J. M. (2013). Complex carbon cycling responses to multi-level warming and supplemental summer rain in a high Arctic ecosystem. *Global Change Biology*, *58*, 701–714. https://doi.org/10.1111/gcb.12149

Spencer, R. G. M., Mann, P. J., Dittmar, T., Eglinton, T. I., McIntyre, C., Holmes, R. M., et al. (2015). Detecting the signature of permafrost thaw in Arctic rivers. *Geophysical Research Letters*, *42*, 2830–2835. https://doi.org/10.1002/2015GL063498

Spencer, R. G. M., Pellerin, B. A., Bergamaschi, B. A., Downing, B. D., Kraus, T. E. C., Smart, D. R., et al. (2007). Diurnal variability in riverine dissolved organic matter composition determined byin situ optical measurement in the San Joaquin River (California, USA). *Hydrological Processes*, *21*(23), 3181–3189. https://doi.org/10.1002/hyp.6887

Stubbins, A., Hood, E., Raymond, P. A., Aiken, G. R., Sleighter, R. L., Hernes, P. J., et al. (2012). Anthropogenic aerosols as a source of ancient dissolved organic matter in glaciers. *Nature Geoscience*, *5*(3), 198–201. https://doi.org/10.1038/ngeo1403

Sullivan, P. F., Welker, J. M., Steltzer, H., Sletten, R. S., Hagedorn, B., Arens, S. J. T., & Horwath, J. L. (2008). Energy and water additions give rise to simple responses in plant canopy and soil microclimates of a high Arctic ecosystem. *Journal of Geophysical Research*, *113*, G03S08. https://doi.org/10.1029/2007JG000477

Tedesco, M., Fettweis, X., Mote, T., Wahr, J., Alexander, P., Box, J. E., & Wouters, B. (2013). Evidence and analysis of 2012 Greenland records from spaceborne observations, a regional climate model and reanalysis data. *The Cryosphere*, *7*(2), 615–630. https://doi.org/10.5194/tc-7-615-2013

Tedesco, M., Mote, T., Fettweis, X., Hanna, E., Jeyaratnam, J., Booth, J. F., et al. (2016). Arctic cut-off high drives the poleward shift of a new Greenland melting record. *Nature Communications*, *7*(1). https://doi.org/10.1038/ncomms11723

Timmermans, M.-L., Toole, J., & Krishfield, R. (2018). Warming of the interior Arctic Ocean linked to sea ice losses at the basin margins. *Science Advances*, *4*(8), eaat6773. https://doi.org/10.1126/sciadv.aat6773

Xu, X., Trumbore, S. E., Zheng, S., Southon, J. R., McDuffee, K. E., Luttgen, M., & Liu, J. C. (2007). Modifying a sealed tube zinc reduction method for preparation of AMS graphite targets: Reducing background and attaining high precision. *Nuclear Instruments and Methods in Physics Research B*, *259*, 320–329. https://doi.org/10.1016/j.nimb.2007.01.175

Yang, Q., Dixon, T. H., Myers, P. G., Bonin, J., Chambers, D., van den Broeke, M. R., et al. (2016). Recent increases in Arctic freshwater flux affects Labrador Sea convection and Atlantic overturning circulation. *Nature Communications*, *7*(1). https://doi.org/10.1038/ncomms10525

Zhu, Z.-Y., Wu, Y., Liu, S.-M., Wenger, F., Hu, J., Zhang, J., & Zhang, R.-F. (2016). Organic carbon flux and particulate organic matter composition in Arctic valley glaciers: Examples from the Bayelva River and adjacent Kongsfjorden. *Biogeosciences*, *13*(4), 975–987. https://doi.org/10.5194/bg-13-975-2016